

Supporting information

**An ultra-tough and ultra-sensitive ionogel pressure/temperature sensor enabled
by hierarchical design of both materials and devices**

*Zong-Ju Chen^{‡,a}, Yu-Qiong Sun^{‡,b}, Xiong Xiao^a, Hong-Qin Wang^a, Min-Hao Zhang^a,
Fang-Zhou Wang^a, Jian-Cheng Lai,^a Da-Shuai Zhang,^c Li-Jia Pan^b, Cheng-Hui Li^{a,*}*

^a State Key Laboratory of Coordination Chemistry, School of Chemistry and Chemical Engineering, Nanjing National Laboratory of Microstructures, Collaborative Innovation Center of Advanced Microstructures, Nanjing University, Nanjing, 210023, China

^b School of Electronic Science and Engineering, National Laboratory of Microstructures, Nanjing University, Nanjing, 210093, China

^c Key Laboratory of Water Pollution Treatment and Resource Reuse of Hainan Province, Haikou, 571158, China

[‡]These authors contributed equally to this work.

* Corresponding author.

E-mail addresses: chli@nju.edu.cn (C. H. Li).

S1. Synthesis of 5-chloro-2-hydroxyisophthalaldehyde

The 5-chloro-2-hydroxyisophthalaldehyde was synthesized according to ref.³⁴ 4-Chlorophenol (12.8 g, 100 mmol) and hexamethylenetetramine (28.0 g, 200 mmol) were dissolved in anhydrous trifluoroacetic acid (200 mL) under argon atmosphere, the resulting solution was refluxed for 24 h, and the color changed from yellow to reddish-orange. The mixture was poured into 4 M HCl (600 mL) and stirred for 5 min, after which the solution was settled for 24 h and yellow crystal precipitated out. The precipitates were collected by filtration and washed with deionized water and hexane. The product was purified by recrystallized in ethyl alcohol. The resulting yellow crystals were filtered off and dried in vacuum oven at 70 °C to give pure 5-chloro-2-hydroxyisophthalaldehyde (8.3 g, yield 45%). ¹H NMR (400 MHz, DMSO, δ): 11.59 (s, 1 H), 10.20 (s, 2 H), 7.99 (s, 2 H).

S2. Synthesis of 2,6-bis((E)-(allylimino)methyl)-4-chlorophenol (Al-Hbimcp)

The Al-Hbimcp and (E)-2-((allylimino)methyl)phenol were synthesized according to ref.³⁴ 5-Chloro-2-hydroxyisophthalaldehyde (1.84 g, 10 mmol) and allylamine hydrochloride (1.87 g, 20 mmol) were dissolved in anhydrous ethanol (40 mL) under stirring, and then acetic acid (200 μ L) was added into the solution as a catalyst. The resulting mixture was stirred for 4 h at 65 °C under argon atmosphere. After the reaction, the solution was concentrated by rotary evaporation at 45 °C and the reddish-orange oil was obtained (2.23 g, yield 85%). ¹H NMR (400 MHz, DMSO, δ): 14.33 (s, 1 H), 8.61 (d, 2 H), 7.46 (dd, 2 H), 6.05 (m, 2 H), 5.20 (m, 4 H), 4.27 (ddt, 4 H).

(E)-2-((allylimino)methyl)phenol was synthesized in the same way. ¹H NMR (400 MHz, DMSO, δ): 10.86 (s, 1H), 8.34 (s, 1H), 7.63 (dd, 1H), 7.48 (ddd, 1H), 7.08 (dd, 1H), 6.91 (t, 1H), 5.90 (m, 1H), 5.32 (m, 2H), 4.44 (d, 1H).

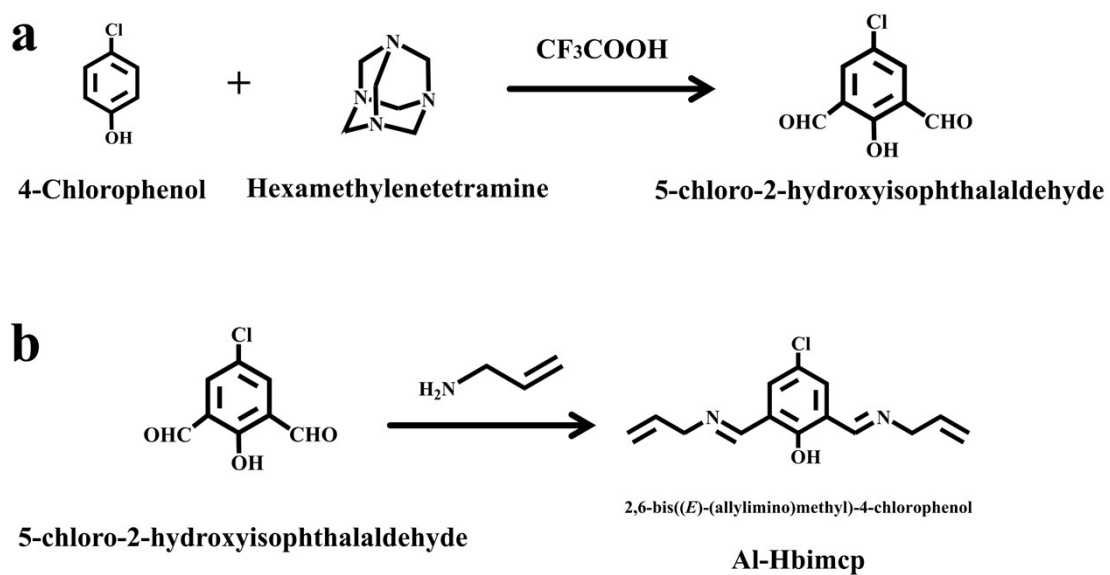


Figure S1. Synthesis of small molecule ligands. (a) Synthesis of 5-chloro-2-hydroxyisophthalaldehyde. (b) Synthesis of 2,6-bis((E)-(allylimino)methyl)-4-chlorophenol.

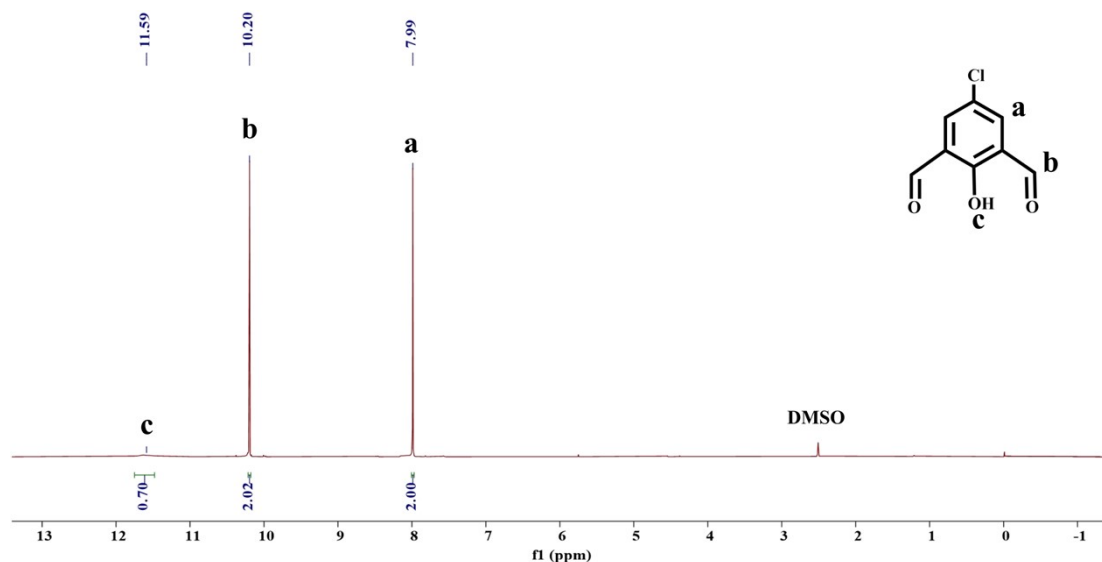


Figure S2. ^1H NMR spectra of 5-chloro-2-hydroxyisophthalaldehyde.

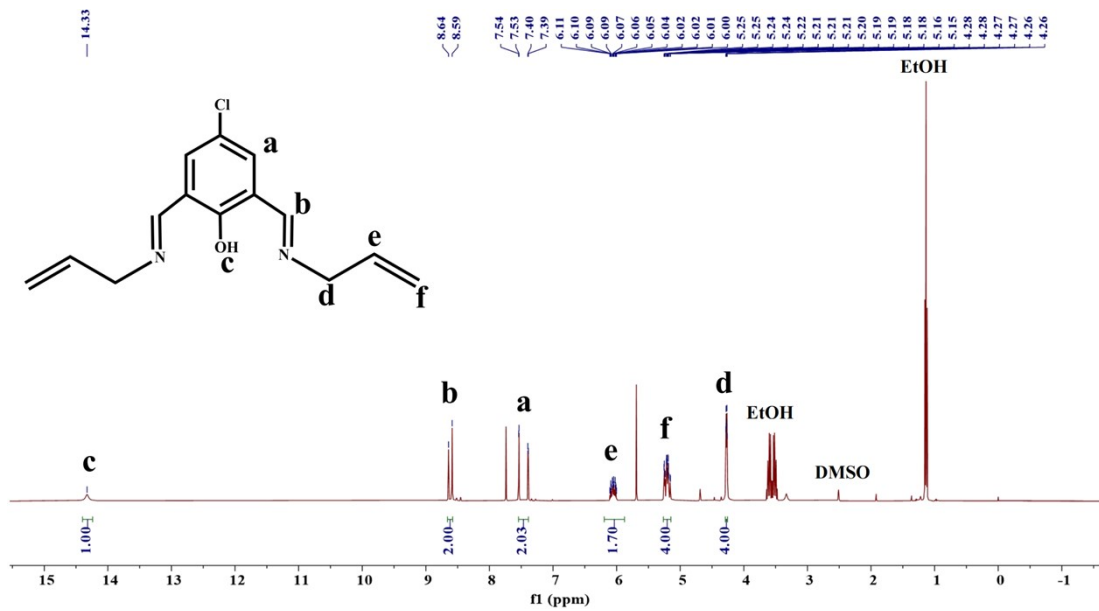


Figure S3. ¹H NMR spectra of Al-Hbimcp.

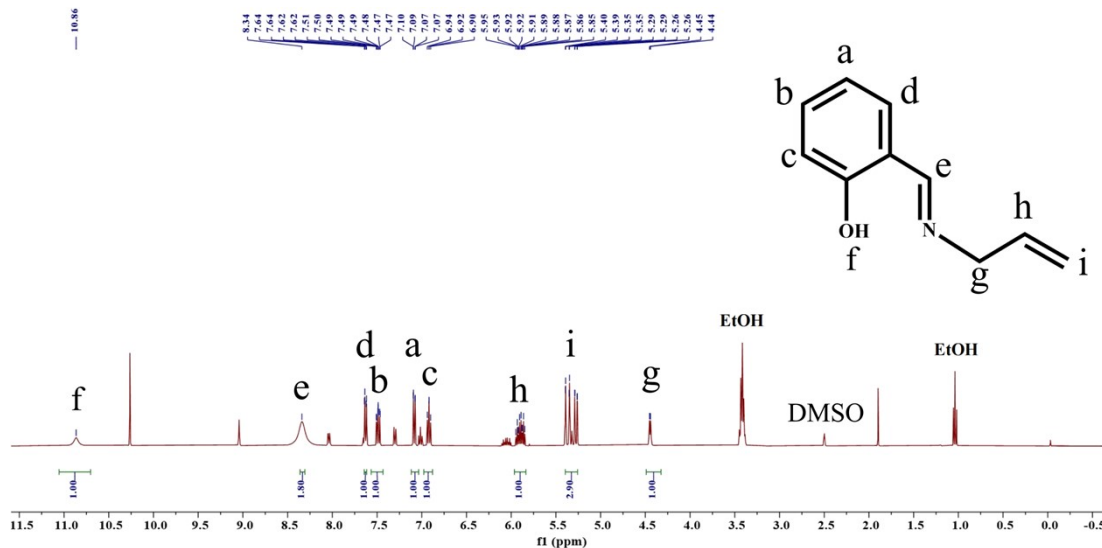


Figure S4. ¹H NMR spectra of (E)-2-((allylimino)methyl)phenol.

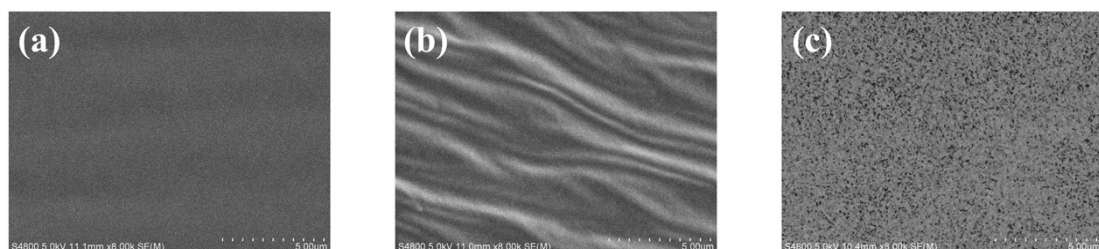


Figure S5. SEM images of (a) pure PAA ionogel, (b) IG_{0.5} and (c) IG_{0.825}-AL_{0.26%}-Zn_{18%}.

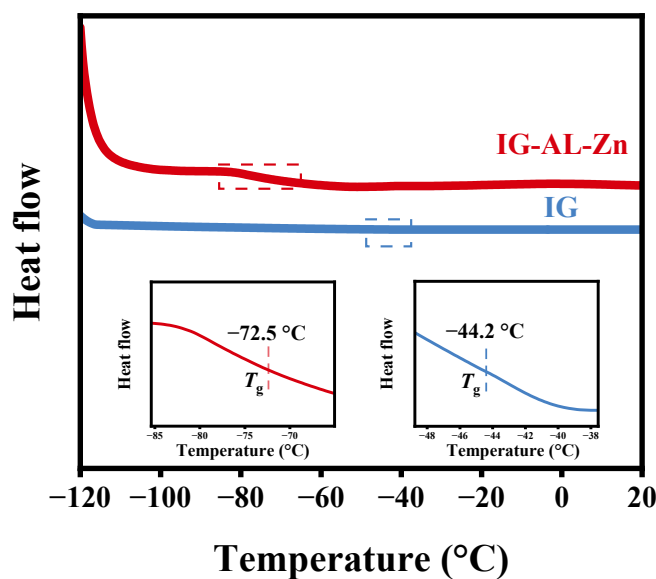


Figure S6. DSC curves of $\text{IG}_{0.825}$ and $\text{IG}_{0.825}\text{-AL}_{0.26\%}\text{-Zn}_{18\%}$.

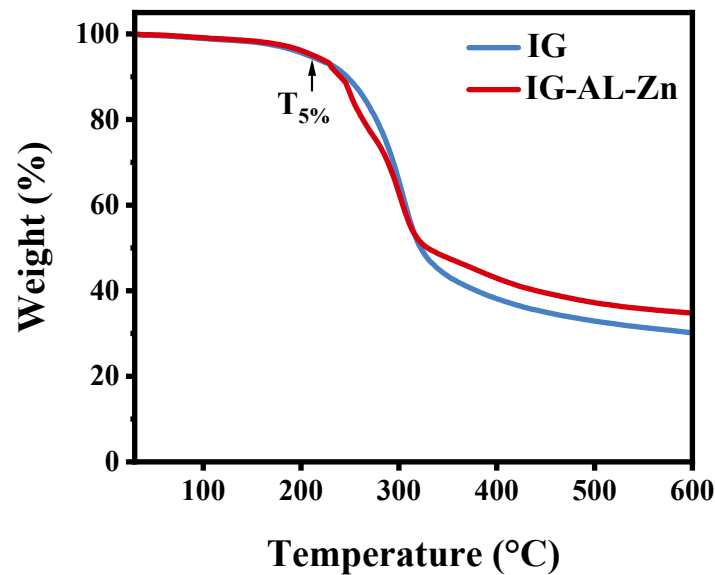


Figure S7. TGA curves of $\text{IG}_{0.825}$ and $\text{IG}_{0.825}\text{-AL}_{0.26\%}\text{-Zn}_{18\%}$.

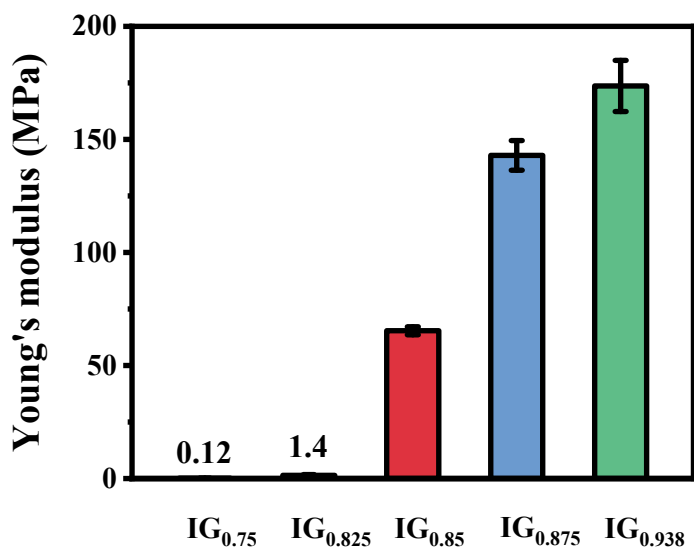


Figure S8. Young's modulus of IG with different monomer compositions.

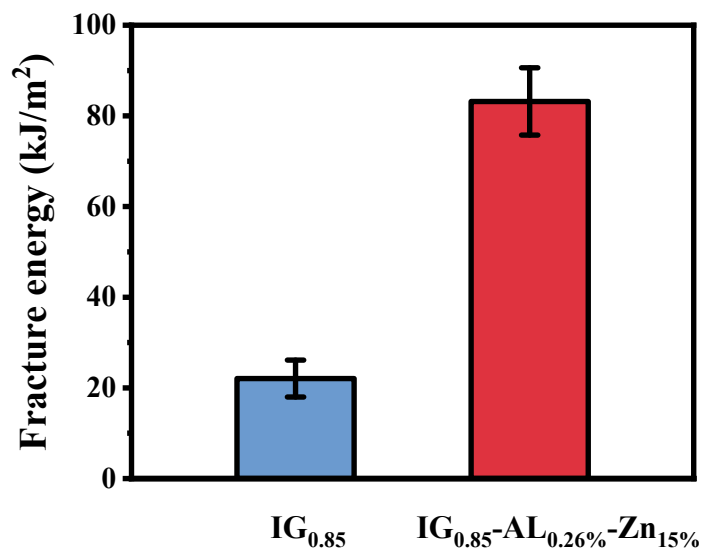


Figure S9. A comparison of fracture energy of $\text{IG}_{0.85}$ and $\text{IG}_{0.85}\text{-AL}_{0.26\%}\text{-Zn}_{15\%}$.

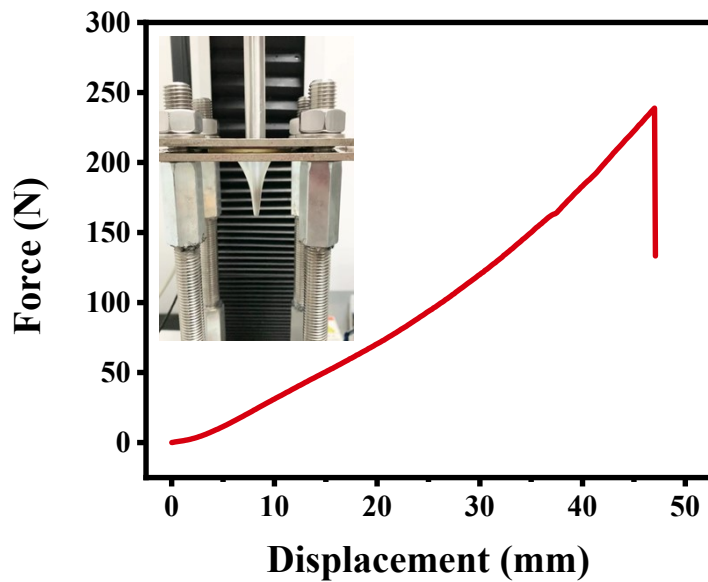


Figure S10. Puncture curves of $\text{IG}_{0.825}\text{-AL}_{0.26\%}\text{-Zn}_{18\%}$ under the deformation rate of 100 mm min^{-1} (1 mm thickness).

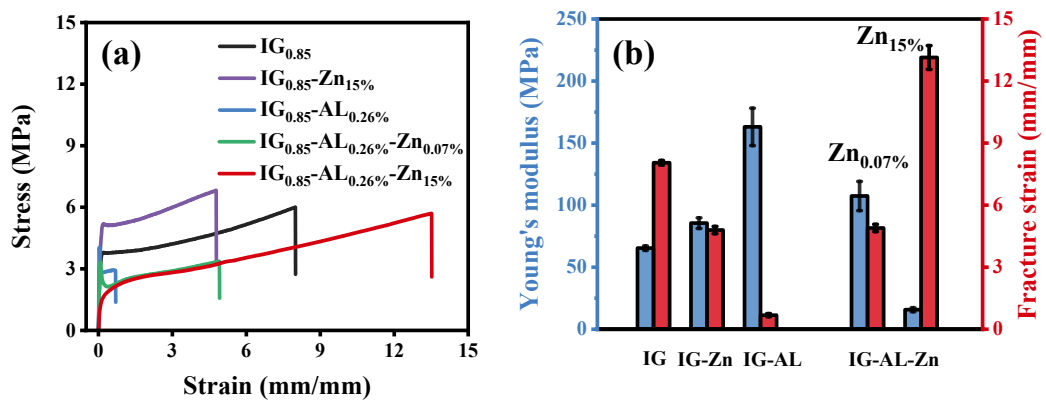


Figure S11. Comparison of (a) strain-stress curves, (b) Young's modulus and fracture strain for $\text{IG}_{0.85}$, $\text{IG}_{0.85}\text{-Zn}_{15\%}$, $\text{IG}_{0.85}\text{-AL}_{0.26\%}$, $\text{IG}_{0.85}\text{-AL}_{0.26\%}\text{-Zn}_{0.07\%}$ and $\text{IG}_{0.85}\text{-AL}_{0.26\%}\text{-Zn}_{15\%}$.

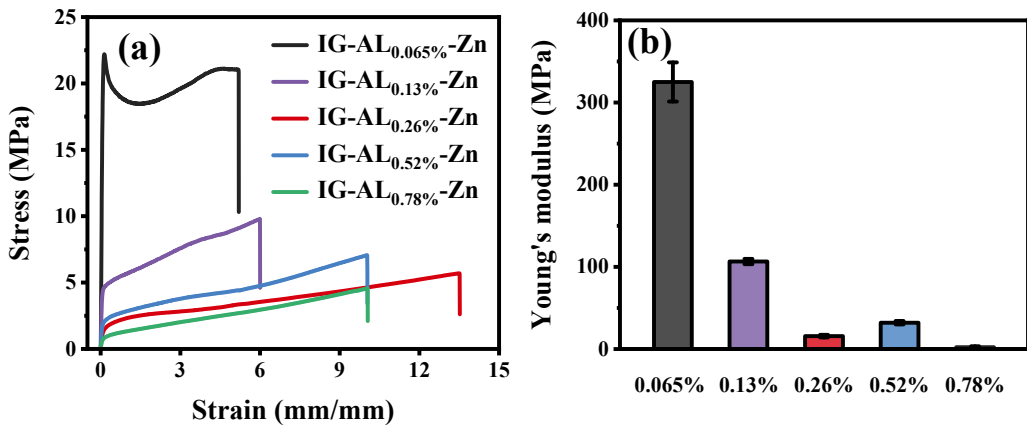


Figure S12. (a) Tensile strain-stress curves and (b) Young's modulus of $\text{IG}_{0.85}\text{-AL-Zn}_{15\%}$ with different Al-Hbimcp contents.

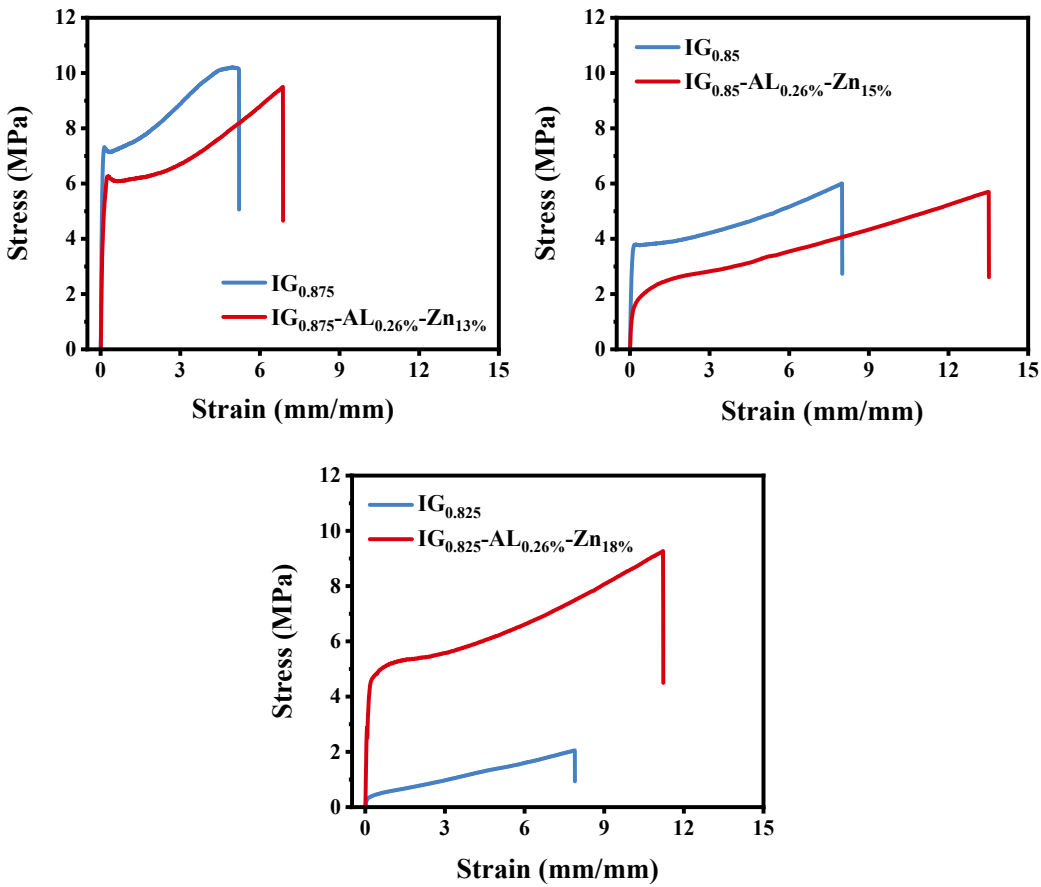


Figure S13. Tensile strain-stress curves of ionogels before and after adding $[\text{Zn}(\text{Al-Hbimcp})_2]^{2+}$.

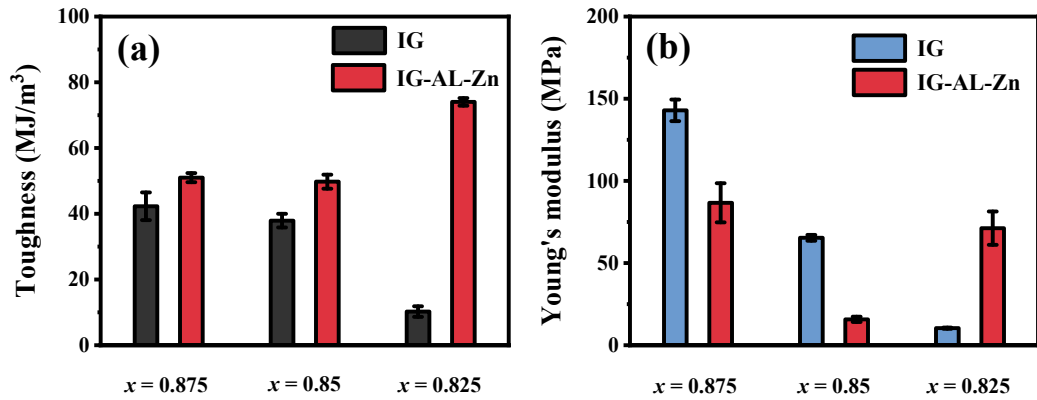


Figure S14. (a) Toughness and (b) Young's modulus of ionogels before and after adding $[\text{Zn}(\text{Al-Hbimcp})_2]^{2+}$.

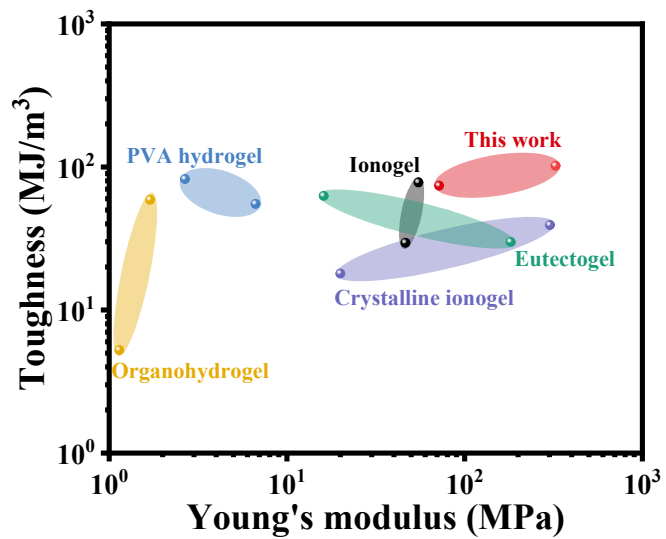


Figure S15. Comparison between this work and various gels in terms of toughness in relation to Young's modulus. Gels include IG-AL-Zn ionogels in this work, PVA hydrogel,^{S1,S2} organohydrogel,^{S3,S4} eutectogel,^{S5,S6} ionogel^{S7,S8} and Crystalline ionogel.^{S9,S10}

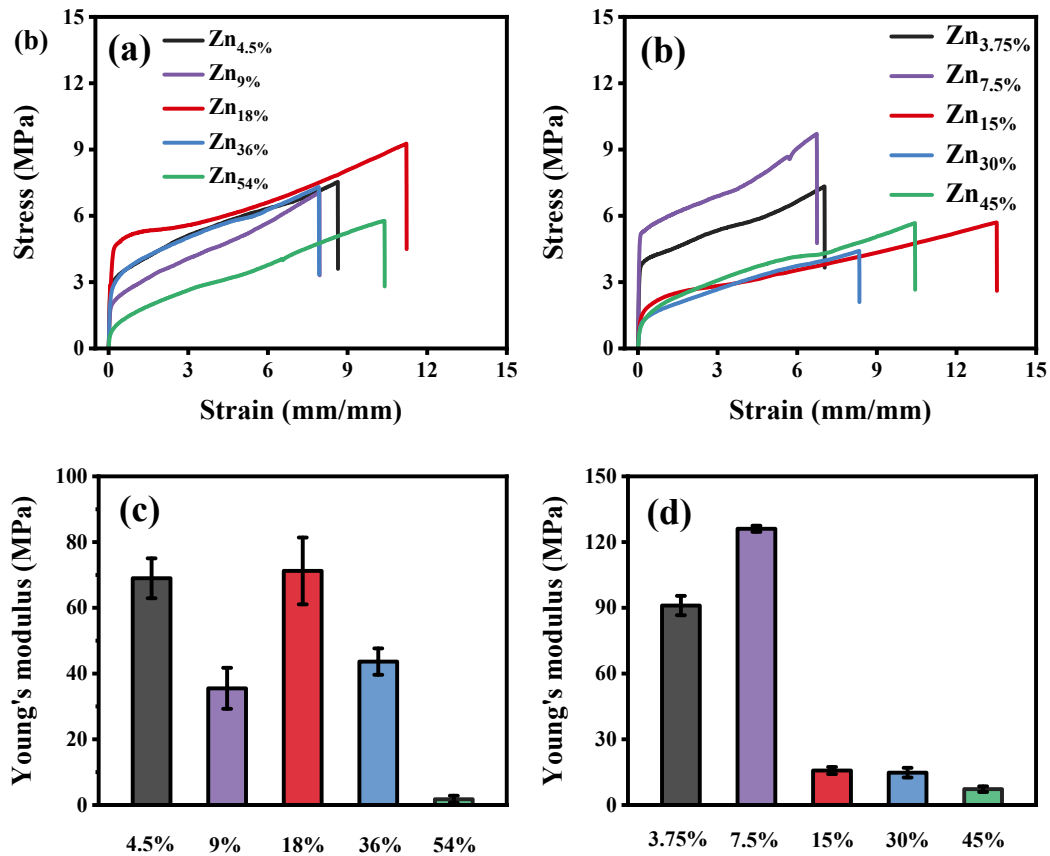


Figure S16. (a–b) Tensile strain-stress curves and (c–d) Young's modulus of $\text{IG}_{0.825}\text{-AL}_{0.26\%}\text{-Zn}$ and $\text{IG}_{0.85}\text{-AL}_{0.26\%}\text{-Zn}$ with different ZnCl_2 contents.

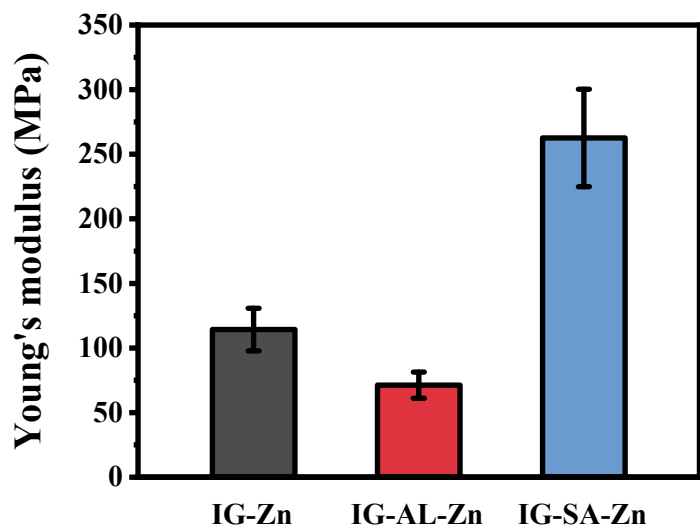


Figure S17. Young's modulus of $\text{IG}_{0.825}\text{-Zn}_{18\%}$, $\text{IG}_{0.825}\text{-AL}_{0.26\%}\text{-Zn}_{18\%}$ and $\text{IG}_{0.825}\text{-SA}_{0.16\%}\text{-Zn}_{18\%}$.

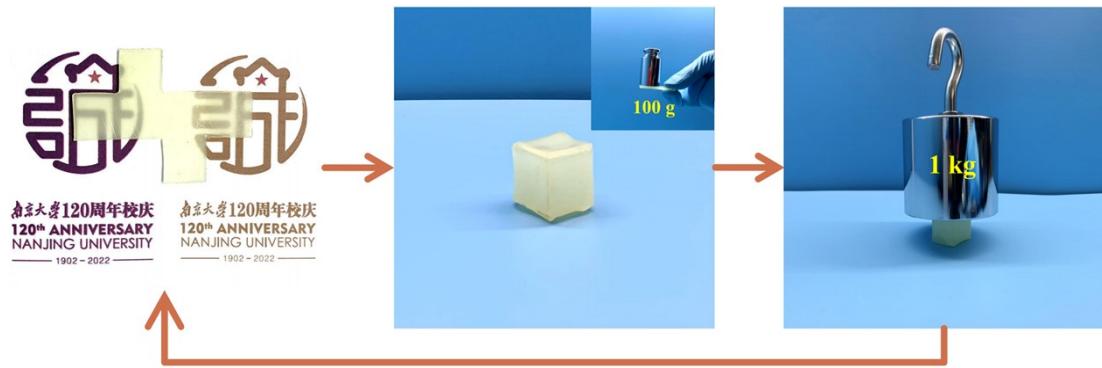


Figure S18. The ionogel ($\text{IG}_{0.85}\text{-AL}_{0.065\%}\text{-Zn}_{15\%}$) was folded into a cube with a side length of 1.5 cm to support a 1 kg weight. It was subsequently unfolded back to its initial shape by its shape memory property at 80 °C.



Figure S19. Adhesion behavior of $\text{IG}_{0.825}\text{-AL}_{0.26\%}\text{-Zn}_{18\%}$ on PTFE.

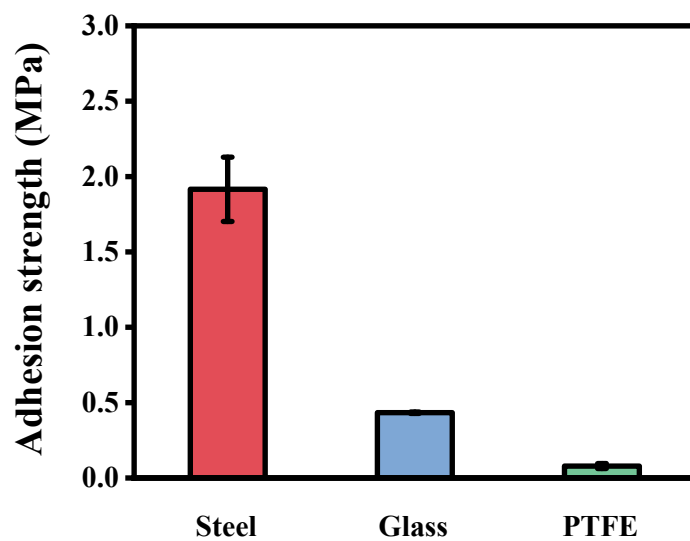


Figure S20. The adhesion strength of $\text{IG}_{0.825}\text{-AL}_{0.26\%}\text{-Zn}_{18\%}$ on different substrates.

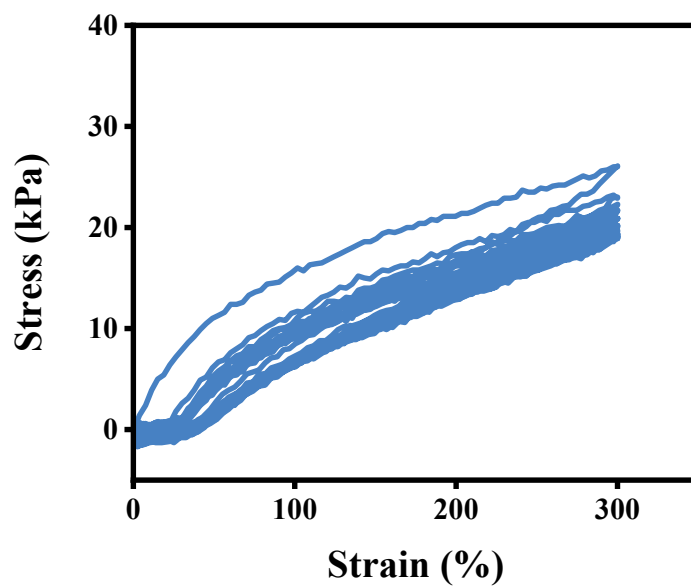


Figure S21. Successive 20 cyclic tensile curves of $\text{IG}_{0.5}$ at 300% strain.

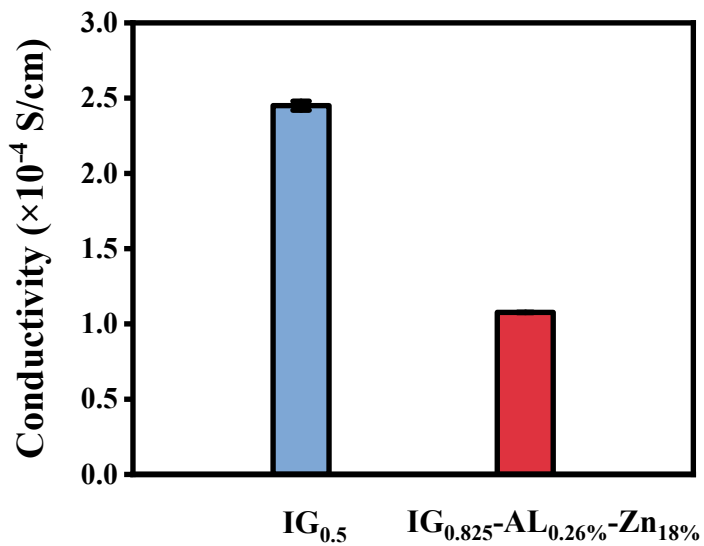


Figure S22. The ionic conductivity of $\text{IG}_{0.5}$ and $\text{IG}_{0.825}\text{-AL}_{0.26\%}\text{-Zn}_{18\%}$.

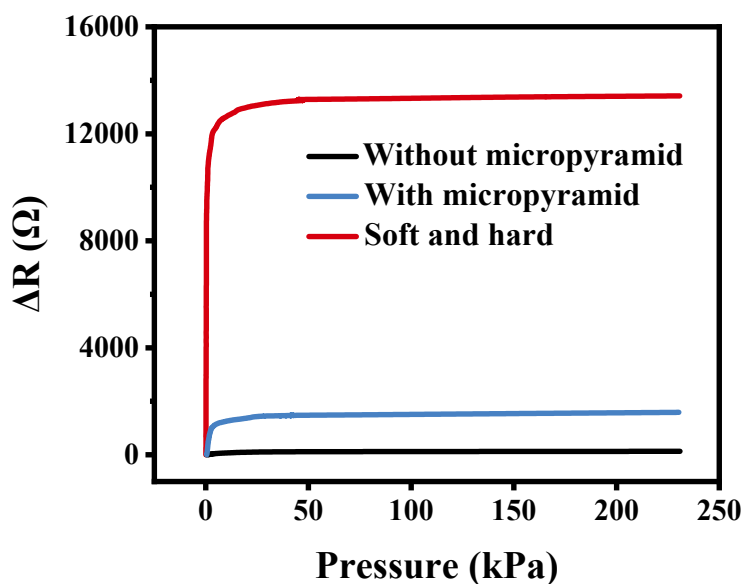


Figure S23. Resistance changes of plain ionogel, soft ionogel with a micro-pyramid structure and bilayer ionogel film sensors under different pressures.

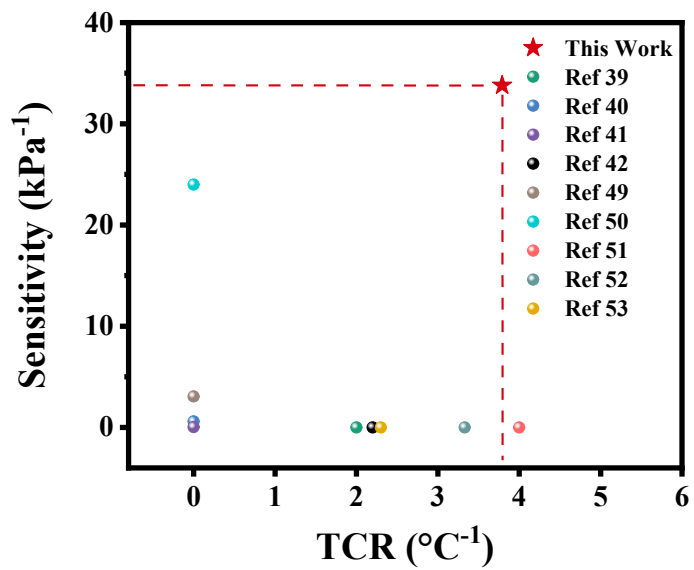


Figure S24. A comparison between this work and the representative piezoresistive ionogel pressure sensors reported in recent years in terms of sensitivity and temperature coefficient of resistance.

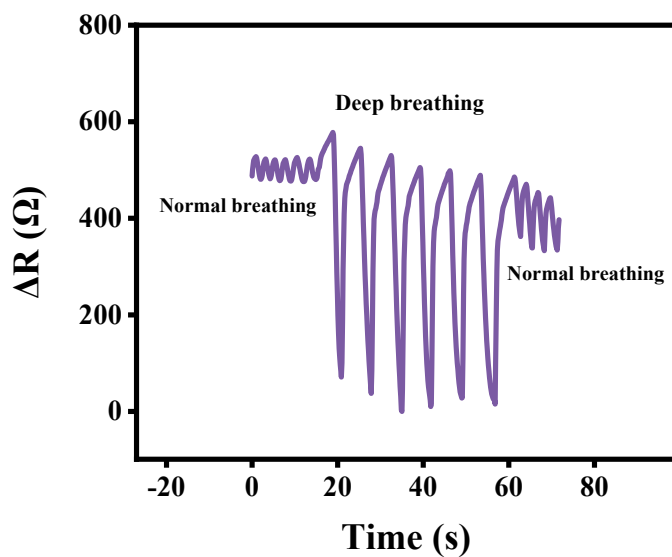


Figure S25. Breathing monitoring.

Table S1. The compositions of various ionogels^a.

Ionogels	AAm (g)	AA (g)	Al-Hbimcp (mg)	ZnCl ₂ (mg)	Stress (MPa)	Strain (%)
IG _{0.5}	0.533	0.54	0	0	0.043	614
IG _{0.75}	0.7988	0.27	0	0	0.59	684
IG _{0.825}	0.8786	0.189	0	0	2.7	797
IG _{0.85}	0.9053	0.162	0	0	6.0	799
IG _{0.875}	0.9319	0.135	0	0	10.2	521
IG _{0.938}	0.9985	0.067	0	0	15.0	577
IG _{0.825} -AL _{0.26%} -Zn _{18%}	0.878	0.189	2.625	179.2	9.3	1120
IG _{0.825} -Zn _{18%}	0.878	0.189	0	178.6	10.4	675
IG _{0.825} -AL _{0.26%}	0.878	0.189	2.625	0	5.4	470
IG _{0.825} -AL _{0.26%} -Zn _{0.07%}	0.878	0.189	2.625	0.681	6.4	739
IG _{0.825} -AL _{0.065%} -Zn _{18%}	0.878	0.189	0.6563	178.7	9.9	608
IG _{0.825} -AL _{0.13%} -Zn _{18%}	0.878	0.189	1.3125	178.9	13.8	583
IG _{0.825} -AL _{0.52%} -Zn _{18%}	0.878	0.189	5.25	179.9	10.4	1110
IG _{0.825} -AL _{0.78%} -Zn _{18%}	0.878	0.189	7.875	180.6	3.5	1134
IG _{0.825} -AL _{0.26%} -Zn _{4.5%}	0.878	0.189	2.625	44.8	7.5	863
IG _{0.825} -AL _{0.26%} -Zn _{9%}	0.878	0.189	2.625	89.6	7.3	784
IG _{0.825} -AL _{0.26%} -Zn _{36%}	0.878	0.189	2.625	358.4	7.3	792
IG _{0.825} -AL _{0.26%} -Zn _{54%}	0.878	0.189	2.625	537.6	5.8	1038
IG _{0.85} -AL _{0.26%} -Zn _{15%}	0.9053	0.162	2.625	154	5.7	1350
IG _{0.85} -Zn _{15%}	0.9053	0.162	0	153.4	6.8	478
IG _{0.85} -AL _{0.26%}	0.9053	0.162	2.625	0	2.9	69
IG _{0.85} -AL _{0.26%} -Zn _{0.07%}	0.9053	0.162	2.625	0.681	3.4	490
IG _{0.85} -AL _{0.065%} -Zn _{15%}	0.9053	0.162	0.6563	153.5	21.0	519
IG _{0.85} -AL _{0.13%} -Zn _{15%}	0.9053	0.162	1.3125	153.7	9.8	600
IG _{0.85} -AL _{0.52%} -Zn _{15%}	0.9053	0.162	5.25	154.7	7.1	1004
IG _{0.85} -AL _{0.78%} -Zn _{15%}	0.9053	0.162	7.875	155.4	4.6	1005

IG _{0.85} -AL _{0.26%} -Zn _{3.75%}	0.9053	0.162	2.625	38.5	7.3	703
IG _{0.85} -AL _{0.26%} -Zn _{7.5%}	0.9053	0.162	2.625	77	9.7	673
IG _{0.85} -AL _{0.26%} -Zn _{30%}	0.9053	0.162	2.625	30.8	4.4	832
IG _{0.85} -AL _{0.26%} -Zn _{45%}	0.9053	0.162	2.625	462	5.7	1043
IG _{0.875} -AL _{0.26%} -Zn _{13%}	0.9319	0.135	2.625	128.1	9.5	686

^{a)} The amounts of EMIES (2 g), MBAA (0.002 g), and I2959 (0.002 g) were not listed in the table as they were kept constant in the experiment. The contents of AAm, AA and EMIES (ionic liquid) were calculated based on 2.5 mL precursor.

Illustration of Supporting Movies

Supplementary Video S1. Video shows the tear resistance of PDMS, soft ionogel and bilayer ionogel film.

Supplementary Video S2. Video shows the puncture resistance of PDMS, soft ionogel and bilayer ionogel film.

References

- [S1] D. Liu, Y. Cao, P. Jiang, Y. Wang, Y. Lu, Z. Ji, X. Wang and W. Liu, *Small*, 2023, DOI: 10.1002/smll.202206819.
- [S2] Y. Wu, Y. Zhang, H. Wu, J. Wen, S. Zhang, W. Xing, H. Zhang, H. Xue, J. Gao and Y. Mai, *Adv. Mater.*, 2023, DOI: 10.1002/adma.202210624.
- [S3] X. Dong, X. Guo, Q. Liu, Y. Zhao, H. Qi and W. Zhai, *Adv. Funct. Mater.*, 2022, **32**, 2203610.
- [S4] Y. Ye, Y. Zhang, Y. Chen, X. Han and F. Jiang, *Adv. Funct. Mater.*, 2020, **30**, 2003430.
- [S5] H. Zhang, N. Tang, X. Yu, M. H. Li and J. Hu, *Adv. Funct. Mater.*, 2022, **32**, 2206305.
- [S6] P. Yao, Q. Bao, Y. Yao, M. Xiao, Z. Xu, J. Yang and W. Liu, *Adv. Mater.*, 2023, DOI: 10.1002/adma.202300114.

- [S7] M. Wang, P. Zhang, M. Shamsi, J. L. Thelen, W. Qian, V. K. Truong, J. Ma, J. Hu and M. D. Dickey, *Nat. Mater.*, 2022, **21**, 359–365.
- [S8] L. Li, W. Li, X. Wang, X. Zou, S. Zheng, Z. Liu, Q. Li, Q. Xia and F. Yan, *Angew. Chem.-Int. Edit.*, **61**, e202212512.
- [S9] T. Li, F. Liu, X. Yang, S. Hao, Y. Cheng, S. Li, H. Zhu and H. Song, *ACS Appl. Mater. Interfaces*, 2022, **14**, 29261–29272.
- [S10] Z. Meng, Q. Liu, Y. Zhang, J. Sun, C. Yang, H. Li, M. Loznik, R. Gostl, D. Chen, F. Wang, N. A. Clark, H. Zhang, A. Herrmann and K. Liu, *Adv. Mater.*, 2022, **34**, 2106208.